https://doi.org/10.5194/egusphere-2026-3633
Preprint. Discussion started: 31 July 2026


# Seasonal nitrate-carbon-oxygen coupling along the Lambayeque coast in the northern Humboldt upwelling system: association with land-based nitrogen pressure

Walter Manuel Hoyos-Alayo[1], Jorge Luis Leiva-Piedra[1], Emilio Ramirez-Juidiaz[2], Jose Lázaro Amaro-Mellado[2]

[1]Departamento de Ingeniería Industrial, Universidad Tecnológica del Perú, Avenida Augusto B. Leguía con la Avenida Hernán Güiner s/n, Chiclayo, 14001, Perú.
[2]Instituto Universitario de Arquitectura y Ciencias de la Construcción (IUACC), Universidad de Sevilla, Reina Mercedes Avenue nº 2, Sevilla, 41012, España.

*Correspondence to*: Walter Manuel Hoyos-Alayo (c23712@utp.edu.pe)

Abstract. Coastal nitrate variability along the northern Humboldt upwelling margin reflects the combined influence of ocean circulation, biological transformation, and land-derived inputs. We examined monthly surface fields from the Copernicus Marine Service for 2022-2025 in two marine sectors adjacent to agricultural drain outlets along the Lambayeque coast, Peru. A northern sector used a 0.25° grid cell with one drain outlet and a southern sector used a 0.25° grid cell with three drain outlets. Nitrate ($NO_3^-$) was analysed with total alkalinity, dissolved inorganic carbon, surface $pCO_2$, chlorophyll a, phytoplankton carbon, net primary production, and dissolved oxygen. Annual rice production and regional urea imports were retained only as contextual indicators of land-based nitrogen pressure. Their four-point annual relationships with marine nitrate were positive but not statistically significant and were interpreted descriptively. Surface $NO_3^-$ generally increased from May to October and remained higher in the southern sector. Within-year correlations showed recurrent positive covariation of $NO_3^-$ with dissolved inorganic carbon and $pCO_2$ and inverse covariation with $O_2$, with the most persistent multivariable structure in the southern sector. These patterns identify a recurrent nitrate-carbon-oxygen structure in an under-studied coastal segment of the Humboldt system. They do not quantify land-to-sea nitrogen flux or establish source attribution, but they show that nitrate variability in Lambayeque must be interpreted together with upwelling variability, carbonate-system behaviour, and oxygenation.

## 1 Introduction

Coastal nitrate variability in eastern boundary upwelling systems results from the superposition of nutrient-rich subsurface water, coastal circulation, biological uptake and regeneration, and land-derived inputs (Paparazzo et al., 2024). These processes determine the timing and persistence of nitrate enrichment and its relationship with oxygen and carbon cycling. Along the Peruvian coast, upwelling and the oxygen minimum zone exert strong controls, so nitrate cannot be interpreted as a direct tracer of a single source (Yari et al., 2023; Kittu et al., 2023; Farias and de la Maza, 2024).

Nitrate ($NO_3^-$) is a mobile fraction of dissolved inorganic nitrogen, but its concentration also reflects mixing, residence time, assimilation, nitrification, denitrification, and hydrodynamic removal (Wang et al., 2023). Joint analysis of $NO_3^-$, total alkalinity, dissolved inorganic carbon (DIC), surface partial pressure of $CO_2$ ($pCO_2$), chlorophyll a, phytoplankton carbon, net primary production (NPP), and dissolved oxygen ($O_2$) indicates whether nutrient variability co-occurs with carbonate-system change, biological response, and oxygen reduction (Kessouri et al., 2021; Santos-Bruña et al., 2025).

Copernicus Marine Service products provide co-located monthly fields for these variables on a consistent spatial grid. This consistency supports exploratory assessment of seasonal and sectoral marine covariability in coastal areas where in situ time series are sparse (Cossarini et al., 2021; Brando et al., 2024; Balakrishnan Nair et al., 2024). The products do not replace field observations, and their spatial resolution limits attribution to individual discharge points.

The Lambayeque coast lies within the northern Humboldt upwelling margin and receives drainage from an irrigated agricultural plain. Rice production requires nitrogen fertiliser, and water management can generate nitrogen losses through runoff, drainage, and leaching (Min et al., 2021; Wang et al., 2024; Zhong et al., 2024; Gbedourorou et al., 2025). Regional rice production and urea imports can therefore provide contextual indicators of land-based nitrogen pressure, but they do not measure fertiliser application, crop nitrogen removal, or nitrogen flux to the ocean.

No previous analysis has examined whether the monthly surface nitrate pattern along Lambayeque is accompanied by coherent changes in carbon, biological, and oxygen variables or whether this structure differs between coastal sectors adjacent to major drain outlets. This study therefore describes surface $NO_3^-$ seasonality in northern and southern marine sectors during 2022-2025, quantifies within-year covariation of $NO_3^-$ with DIC, total alkalinity, $pCO_2$, chlorophyll a, phytoplankton carbon, NPP, and $O_2$, and reports the four-year associations with regional rice production and urea imports as contextual descriptive evidence. The oceanographic contribution is the identification of a recurrent nitrate-carbon-oxygen structure and its sectoral persistence in an under-studied part of the Humboldt system. The analysis does not estimate land-to-sea nitrogen flux or establish causation.

## 2 Methodology

### 2.1 Study design and analysis period

An observational, retrospective, spatiotemporal, and correlational design was used to examine surface marine biogeochemical variability along the Lambayeque coast. The analysis covered 2022-2025, with monthly resolution for marine variables and annual resolution for contextual land-based indicators. Two marine sectors were compared to determine whether nitrate seasonality and nitrate-carbon-oxygen covariability differed along the coast. The design supports description of co-variation but not source attribution or causal inference.

https://doi.org/10.5194/egusphere-2026-3633
Preprint. Discussion started: 31 July 2026


## 2.2 Spatial delimitation and extraction of marine-coastal variables

Monthly surface biogeochemical fields were obtained from the Copernicus Marine Service Global Ocean Biogeochemistry Analysis and Forecast product. The product uses a regular 0.25° × 0.25° longitude-latitude grid. The variables were $NO_3^-$, total alkalinity, dissolved inorganic carbon (DIC), surface $pCO_2$, chlorophyll a, phytoplankton carbon, net primary production (NPP), and $O_2$. $NO_3^-$ was expressed in mmol $m^{-3}$ and was the focal marine state variable.

The northern marine sector was represented by the Copernicus grid cell containing the Drain 1000 outlet (80.125989° W, 6.728102° S). The southern marine sector was represented by the common grid cell containing the outlets of drains 1600 (79.909259° W, 6.904548° S), 1700 (79.896899° W, 6.911414° S), and 4000 (79.937411° W, 6.881888° S). The service returned identical marine values for the three southern drain outlets because they fall within the same product grid cell. The southern values were retained once and were not treated as independent replicates. Figure 1 shows the outlet coordinates and the approximate grid cells used to define both sectors.

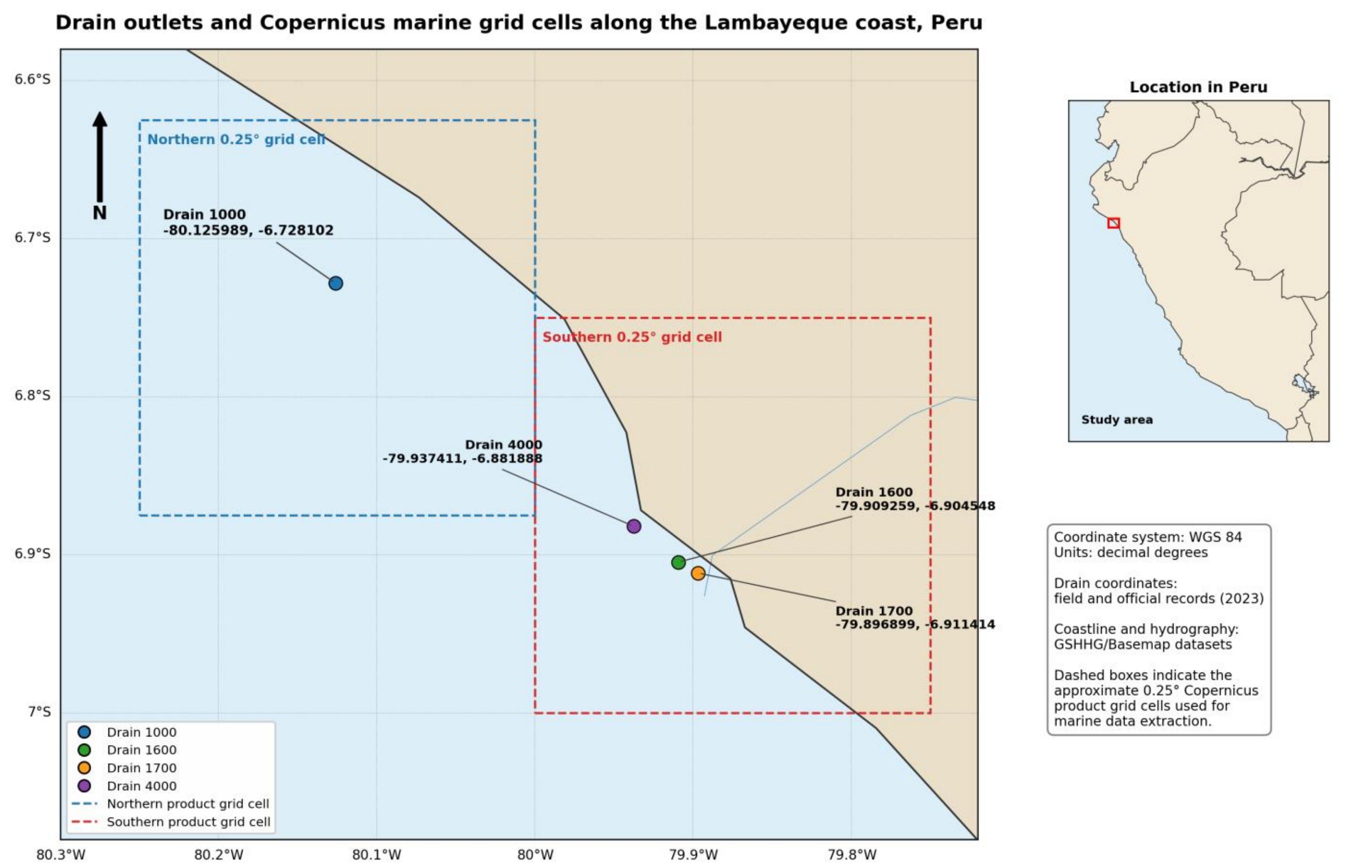


**Figure 1: Drain outlet coordinates and approximate 0.25° Copernicus product grid cells used to define the northern and southern marine sectors along the Lambayeque coast, Peru. Coordinates are in WGS 84.**

https://doi.org/10.5194/egusphere-2026-3633
Preprint. Discussion started: 31 July 2026


The marine dataset was recorded as E.U. Copernicus Marine Service Information, Global Ocean Biogeochemistry Analysis and Forecast, Product ID GLOBAL_ANALYSISFORECAST_BGC_001_028, DOI 10.48670/moi-00015. The monthly datasets were cmems_mod_glo_bgc-nut_anfc_0.25deg_P1M-m for $NO_3^-$, cmems_mod_glo_bgc-car_anfc_0.25deg_P1M-m for total alkalinity and DIC, cmems_mod_glo_bgc-co2_anfc_0.25deg_P1M-m for surface $pCO_2$, cmems_mod_glo_bgc-pft_anfc_0.25deg_P1M-m for chlorophyll a and phytoplankton carbon, and cmems_mod_glo_bgc-bio_anfc_0.25deg_P1M-m for $O_2$ and NPP. Three-dimensional variables were extracted from the first available model depth layer, whereas surface $pCO_2$ was extracted as a two-dimensional surface variable. The subset was downloaded from the Copernicus Marine Data Store on 12 January 2026 and retained the available monthly records from 2022 to 2025 at the drain outlet coordinates (E.U. Copernicus Marine Service Information, 2026).

### 2.3 Agricultural information sources

Annual rice production and regional urea imports were included only as contextual indicators of land-based agricultural activity. Rice production was expressed in metric tonnes. Urea imports represented regional fertiliser availability, not the amount applied to rice fields. The dataset contains no field application rates, crop nitrogen content, drainage discharge, or nitrogen concentration in drain water. A nitrogen surplus or flux to the sea was therefore not calculated.

### 2.4 Temporal harmonisation and consistency control

For each sector, records were matched directly by year and month so that $NO_3^-$ and all companion variables referred to the same grid cell and monthly time step. Units, duplicate records, and missing months were checked. The northern series contained 12 monthly values per year. The southern series used 11 monthly values per year, from February to December. January was absent from the archived southern series used in the submitted analysis and no value was imputed. Annual mean $NO_3^-$ was calculated from the available monthly values for the descriptive comparisons with annual land-based indicators.

### 2.5 Statistical analysis

Pearson correlations were calculated for three purposes. First, annual rice production was compared with annual urea imports. Second, annual rice production was compared with annual mean surface $NO_3^-$ in each marine sector. Each calculation used four paired annual observations, one for each calendar year from 2022 to 2025. For the conventional significance test of Pearson's r, the degrees of freedom equal $n - 2$; therefore, $n = 4$ yields 2 degrees of freedom. Because four successive annual observations do not support a robust independence assumption or reliable inference, the two-sided p values are reported only as descriptive diagnostics. Third, within each year and sector, monthly $NO_3^-$ was correlated with total alkalinity, NPP, DIC, chlorophyll a, $pCO_2$, phytoplankton carbon, and $O_2$. These calculations used $n = 12$ in the northern sector and $n = 11$ in the southern sector. The monthly observations form time series and were not assumed to be fully independent. The reported p values are nominal Pearson p values and were not adjusted for temporal autocorrelation. Interpretation therefore emphasises effect direction, magnitude, and recurrence across years and avoids causal statements.

https://doi.org/10.5194/egusphere-2026-3633
Preprint. Discussion started: 31 July 2026


### 2.6 Graphical representation and interpretation

Figures 2-4 show the descriptive annual associations. Figure 5 shows monthly $NO_3^-$ dynamics. Figures 6 and 7 show within-year Pearson coefficients and nominal p values for the northern and southern sectors. All figures are interpreted as descriptions of co-variation. They do not identify nitrogen sources, quantify land-to-sea flux, or separate agricultural forcing from upwelling and coastal circulation.

## 3 Results

The results begin with the contextual annual indicators, followed by the monthly marine nitrate pattern and the within-year nitrate associations with carbon, biological, and oxygen variables. The annual analyses are descriptive because they contain four observations. The monthly analyses show co-variation within the Copernicus surface fields and are interpreted with the temporal dependence limitation stated in Sect. 2.5.

### 3.1 Contextual annual indicators of land-based nitrogen pressure

Figure 2 shows positive but non-significant interannual covariation between rice production and regional urea imports during 2022-2025 ($r = 0.902$; $R^2 = 81.42\%$; $n = 4$; $p = 0.098$). Because only four annual values are available, this relation is reported as context for land-based nitrogen pressure and not as evidence of fertiliser application or nitrogen delivery to the sea.
The dataset does not include urea applied to rice fields, nitrogen removed in harvested grain, drainage discharge, or nitrogen concentration in drain water. A nitrogen surplus or land-to-sea flux therefore cannot be calculated. The annual indicators are retained only to describe years of relatively higher or lower regional agricultural activity.

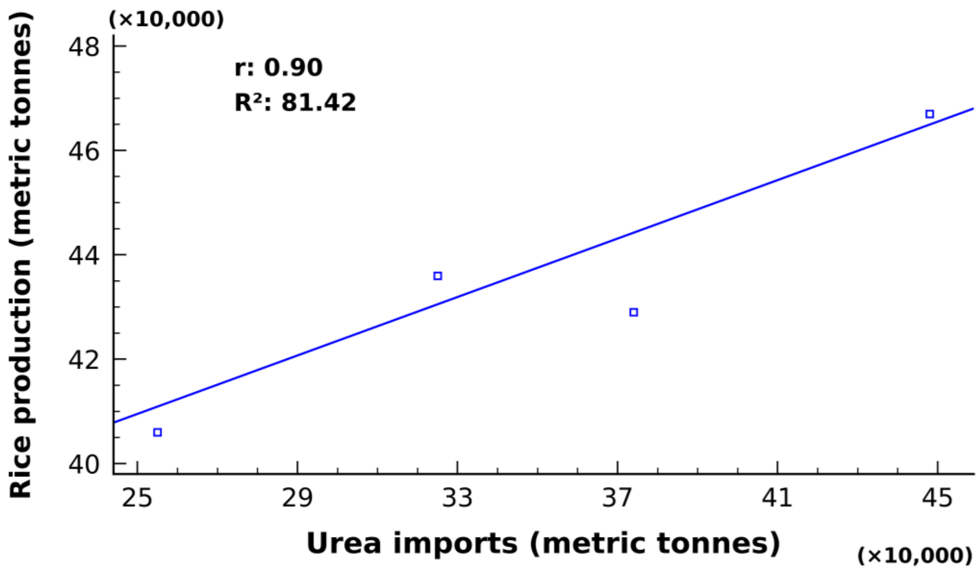


**Figure 2: Descriptive annual relationship between rice production and regional urea imports in Lambayeque, 2022-2025.**

https://doi.org/10.5194/egusphere-2026-3633
Preprint. Discussion started: 31 July 2026


### 3.2 Annual marine nitrate means and land-based indicators

Figure 3 shows a positive but non-significant relationship between rice production and annual mean surface $NO_3^-$ in the northern sector (r = 0.901; $R^2$ = 81.19%; n = 4; p = 0.099). The four values indicate co-variation across the study years, but they do not establish connectivity between rice production and marine nitrate.

Surface $NO_3^-$ in this sector is also influenced by upwelling, mixing, local circulation, biological uptake, and internal nitrogen cycling. The annual comparison is therefore retained only as contextual evidence and is not used for source attribution.

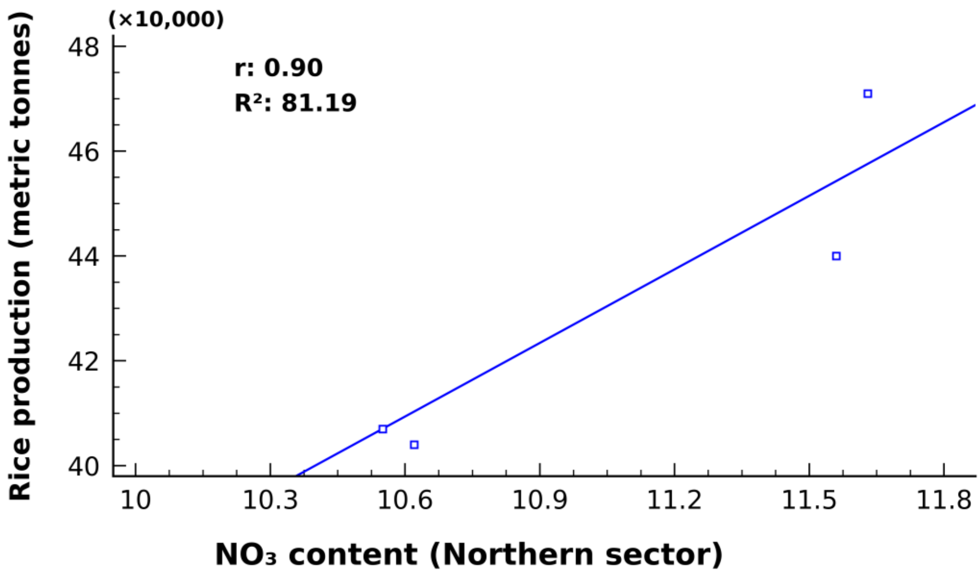


**Figure 3: Descriptive relationship between rice production and annual mean surface nitrate ($NO_3^-$) in the northern marine sector, 2022-2025. $NO_3^-$ is expressed in mmol $m^{-3}$.**

Figure 4 shows a comparable positive but non-significant relationship in the southern sector (r = 0.904; $R^2$ = 81.68%; n = 4; p = 0.096). The four values show co-variation across the study years but do not establish connectivity between rice production and marine nitrate.

The small difference in $R^2$ between sectors does not demonstrate a difference in forcing. It indicates that annual mean $NO_3^-$ covaried similarly with the regional production indicator within the four-year record. Physical and biogeochemical mechanisms cannot be separated with these annual data.

https://doi.org/10.5194/egusphere-2026-3633
Preprint. Discussion started: 31 July 2026


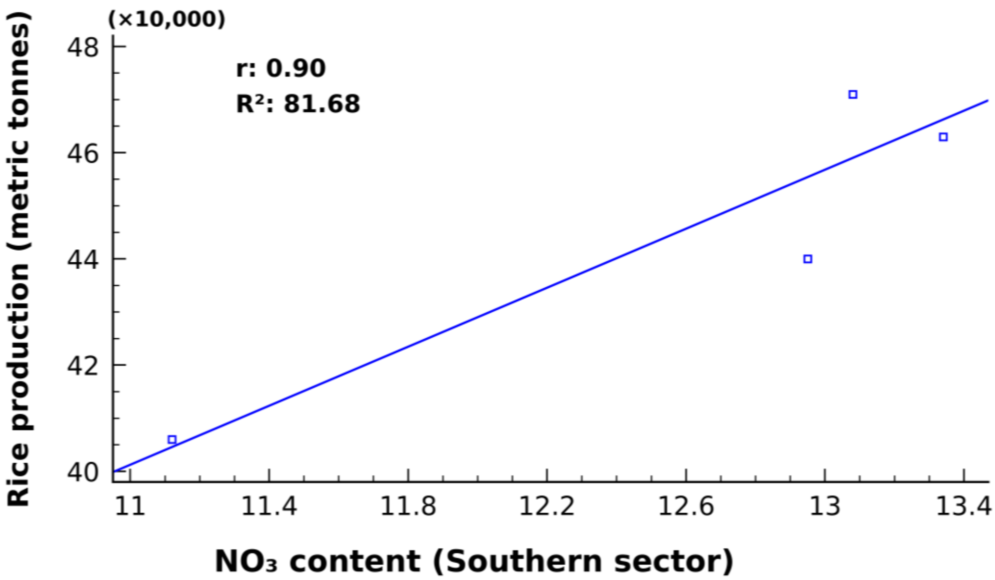


**Figure 4: Descriptive relationship between rice production and annual mean surface nitrate ($NO_3^-$) in the southern marine sector, 2022-2025. $NO_3^-$ is expressed in mmol $m^{-3}$.**

### 3.3 Nitrate content in the northern and southern marine sectors (2022-2025)

Figure 5 shows monthly surface $NO_3^-$ for 2022-2025. The northern series covers January to December, while the southern series covers February to December. In both sectors, $NO_3^-$ generally increased from May to October, with year-specific maxima and declines later in the year. This seasonal structure is compatible with combined changes in upwelling, mixing, biological demand, and external inputs, but the data do not isolate their relative contributions.

The southern sector maintained higher and more persistent $NO_3^-$ during much of the middle of the year, while the northern sector showed larger interannual differences in the timing and magnitude of peaks. This contrast identifies sectoral structure within the model product. It does not by itself indicate greater agricultural exposure or a specific transport pathway.

https://doi.org/10.5194/egusphere-2026-3633
Preprint. Discussion started: 31 July 2026


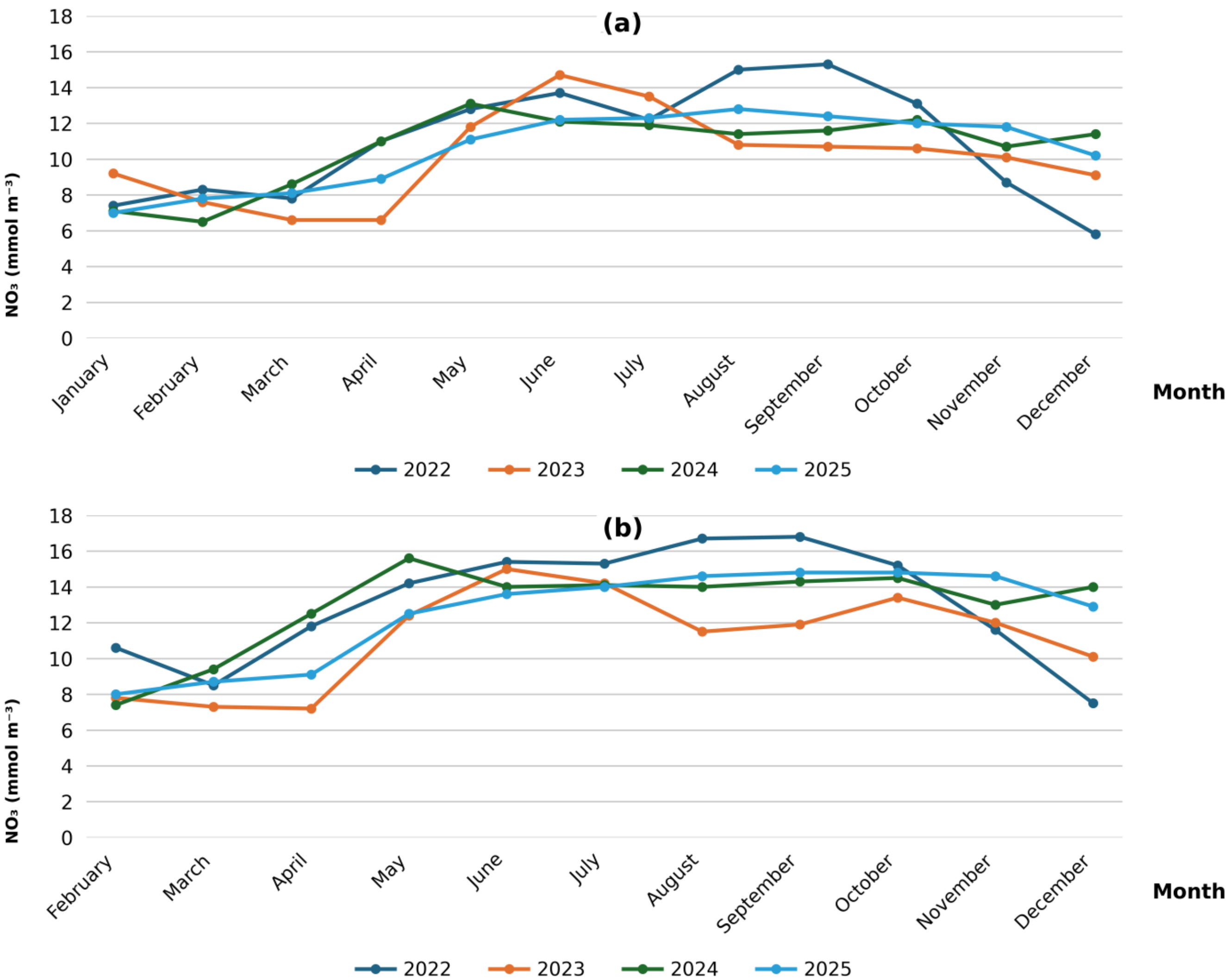


**Figure 5: Monthly surface nitrate ($NO_3^-$) in the marine sectors along the Lambayeque coast during 2022-2025: (a) northern sector and (b) southern sector. The northern panel contains 12 monthly values per year. The southern panel contains 11 values per year, from February to December. $NO_3^-$ is expressed in mmol $m^{-3}$.**

### 3.4 Association of nitrate content with the marine-coastal ecosystem

#### 3.4.1 Northern sector

Figure 6 shows recurrent positive covariation between $NO_3^-$ and DIC in the northern sector, with r values from 0.614 to 0.918. The nominal p values were below 0.05 in each year. Surface $pCO_2$ showed positive covariation in 2022-2024 (r = 0.834-0.869) and a weak relation in 2025 (r = 0.135; nominal p = 0.676). These coefficients describe monthly co-variation within the product fields and do not establish that nitrate caused the carbon-system changes.

https://doi.org/10.5194/egusphere-2026-3633
Preprint. Discussion started: 31 July 2026


$O_2$ showed inverse correlations with $NO_3^-$ in each year (r = -0.711 to -0.947), with nominal p values below 0.05. NPP, chlorophyll a, and phytoplankton carbon showed stronger positive relations in 2024 and 2025 than in the first two years. The pattern indicates that higher-nitrate months often coincided with lower $O_2$ and, in some years, higher biological indicators. The nominal p values do not account for temporal autocorrelation.

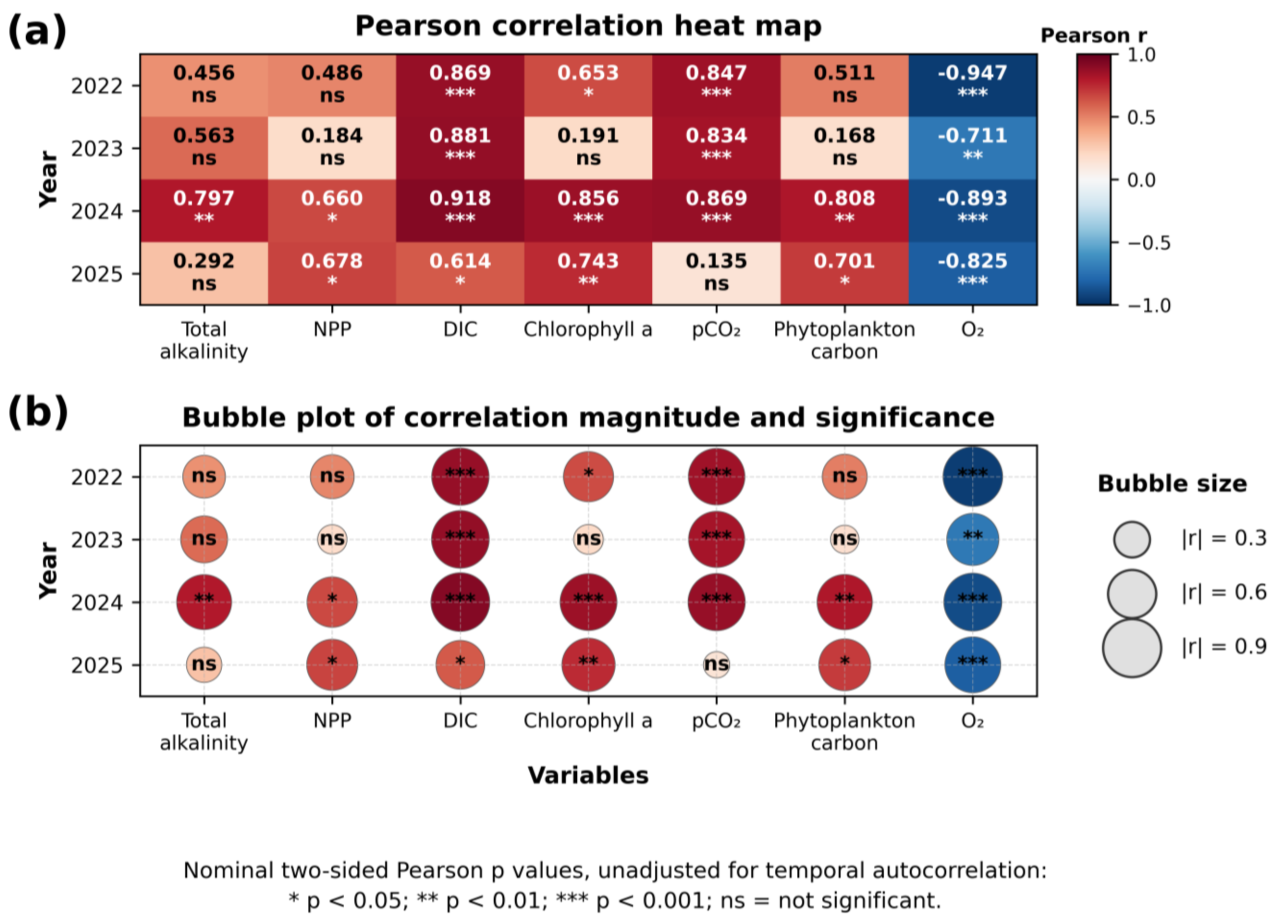


**Figure 6: Pearson correlation heat map (a) and bubble plot (b) for monthly $NO_3^-$ associations in the northern sector (n = 12 per year). Stars indicate nominal two-sided Pearson p values unadjusted for temporal autocorrelation.**

### 3.4.2 Southern sector

Figure 7 shows a more persistent multivariable structure in the southern sector. $NO_3^-$ covaried positively with total alkalinity (r = 0.792-0.906), DIC (r = 0.887-0.954), and $pCO_2$ (r = 0.671-0.930) in all four years, with nominal p values below 0.05. $O_2$ was inversely related to $NO_3^-$ in each year (r = -0.864 to -0.967), with nominal p values below 0.05. NPP, chlorophyll a, and phytoplankton carbon also showed positive relations in 2024 and 2025. Compared with the northern sector, the southern

https://doi.org/10.5194/egusphere-2026-3633
Preprint. Discussion started: 31 July 2026


sector displayed more recurrent nitrate-carbon-oxygen covariation. This is a description of marine co-variability rather than evidence of a single controlling process.

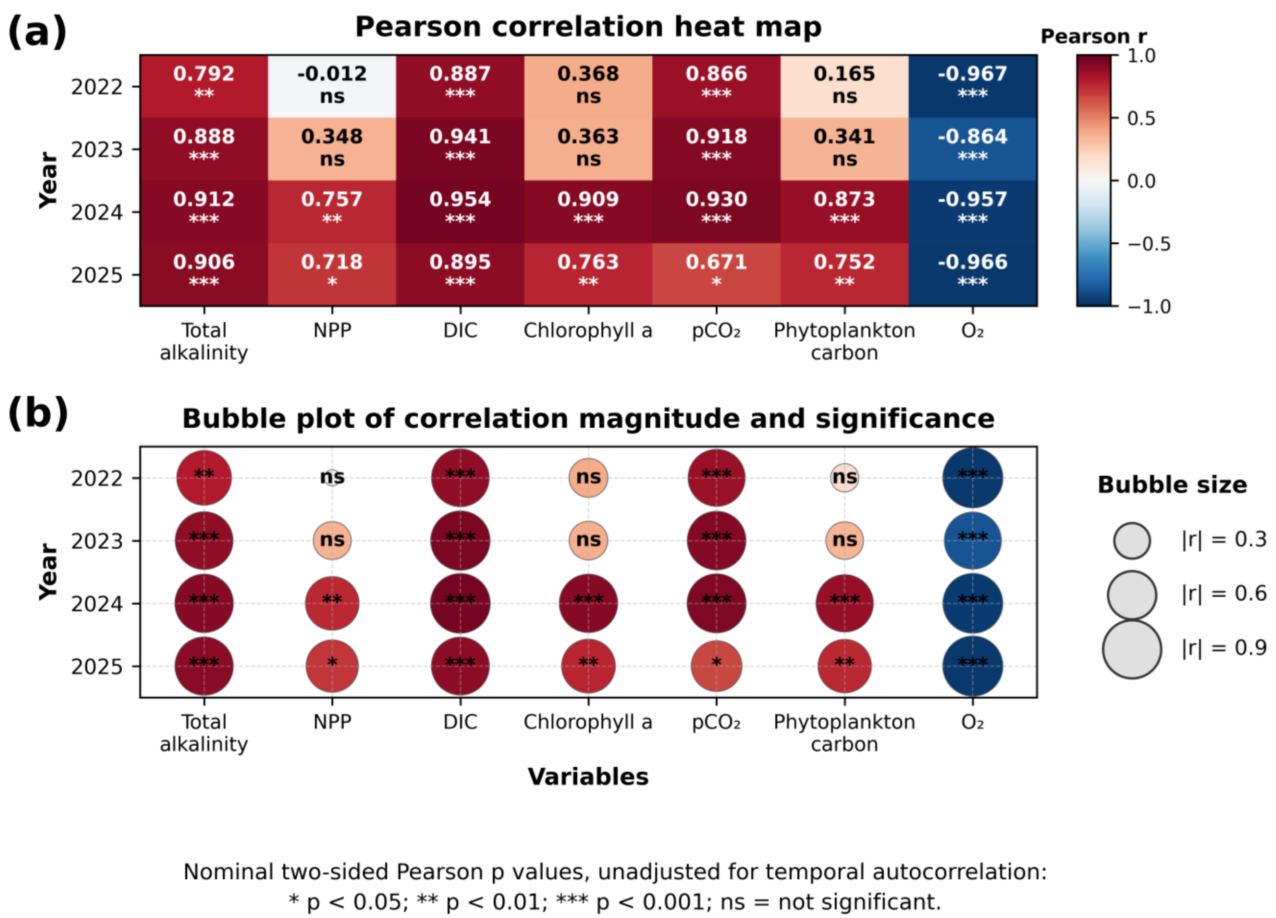


**Figure 7: Pearson correlation heat map (a) and bubble plot (b) for monthly $NO_3^-$ associations in the southern sector (n = 11 per year). Stars indicate nominal two-sided Pearson p values unadjusted for temporal autocorrelation.**

## 4 Discussion

### 4.1 Contextual land-based indicators and limits of source attribution

The annual land-based indicators provide context rather than a nitrogen-input estimate. Rice production and urea imports covaried positively, but the relation was not significant at $p < 0.05$ and contained only four annual observations. Urea imports also represent regional availability rather than fertiliser applied to rice fields. The general concern that inefficient fertiliser use can contribute to nitrate pollution is well established (Bijay-Singh and Craswell, 2021; Peñuelas et al., 2023), but the present analysis does not interpret Figure 2 as evidence of a quantified nitrogen load.

https://doi.org/10.5194/egusphere-2026-3633
Preprint. Discussion started: 31 July 2026


A land-to-sea nitrogen balance would require fertiliser application by crop and season, nitrogen removed in harvested biomass, soil storage and transformation, drainage discharge, and nitrogen concentration in drainage water. None of these components is available in the present dataset. Subtracting rice production from urea imports would not provide a valid nitrogen surplus because the variables have different material bases and spatial coverage. The land indicators are retained only to identify years of relatively higher or lower regional agricultural activity.

### 4.2 Spatial differentiation of the nitrate response

Figures 3 and 4 show similar positive annual co-variation between the land indicator and marine $NO_3^-$, but both relations are non-significant and based on n = 4. The slightly higher $R^2$ in the southern sector does not confirm dependence on transport, residence time, mixing, or hydrodynamic removal. The evidence supports only the statement that annual mean nitrate differed between sectors and covaried with the regional indicator over the same four years.

The monthly pattern in Figure 5 provides the stronger oceanographic result. $NO_3^-$ generally increased from May to October in both sectors, which overlaps the seasonal variability expected in the North Humboldt Upwelling System. Wind-driven upwelling can supply nutrient-rich subsurface water to the euphotic layer (Yari et al., 2023), and nitrate distributions in the Peruvian Upwelling System vary across seasonal, spatial, and interannual scales (Asto et al., 2025). Land-derived nitrogen may contribute to this pattern, but the present data cannot separate it from upwelling, mixing, or internal cycling.

The sectoral contrast adds information for an under-studied part of the Peruvian margin. The southern surface field showed more persistent nitrate and stronger nitrate-carbon-oxygen covariation than the northern field. Regional nitrogen cycling includes simultaneous input and removal processes (Kittu et al., 2023), while carbon and greenhouse-gas pathways respond to physical forcing and oxygen conditions in coastal upwelling systems (Lachkar et al., 2024). The Lambayeque results therefore define a testable oceanographic pattern rather than a source-specific mechanism.

### 4.3 Coupling between nitrate, the carbonate system and biological response

Figures 6 and 7 show recurrent covariation of $NO_3^-$ with DIC and $pCO_2$, especially in the southern sector. This joint behaviour indicates that nitrate-rich months also differed in carbonate-system state within the model fields. It does not show that nitrate directly caused the carbon changes. Coastal eutrophication can intensify acidification and oxygen loss in upwelling systems (Kessouri et al., 2021), and eutrophication assessment benefits from joint analysis of nutrients, plankton, and carbonate-system descriptors (Santos-Bruña et al., 2025). The Lambayeque pattern is consistent with the need for this multivariable interpretation.

The biological response was less consistent than the carbon response. NPP, chlorophyll a, and phytoplankton carbon showed the clearest positive relations with $NO_3^-$ in 2024 and 2025. Nutrient availability does not determine biomass alone because light, mixing, residence time, grazing, nutrient ratios, and seasonal hydrography also regulate biological production. Satellite and operational ocean products can capture broad chlorophyll variability (Li et al., 2024; Brando et al., 2024). In this study,

https://doi.org/10.5194/egusphere-2026-3633
Preprint. Discussion started: 31 July 2026


the biological variables show whether higher-nitrate months also coincide with changes in production and phytoplankton-related fields.

### 4.4 Oxygen response and ecological significance

The inverse relation between $NO_3^-$ and $O_2$ is the most recurrent marine signal in the study. $O_2$ was negatively related to $NO_3^-$ in every year and in both sectors, with stronger coefficients in the southern sector. The analysis does not demonstrate hypoxia because no in situ threshold assessment was performed. It shows that, within the monthly surface fields of the 0.25° model product, higher-nitrate months tended to coincide with lower $O_2$. Coastal deoxygenation is linked with nitrogen cycling in eastern boundary upwelling systems (Farias and de la Maza, 2024), and riverine organic matter can contribute indirectly to oxygen loss (Zhang, 2022).

These relations support joint monitoring of nitrate, oxygen, and carbon variables, but they do not establish a nitrate-driven mechanism. Nitrate enrichment can accompany organic-matter production and respiration, while upwelled waters can also contain high nutrients and low oxygen. Cheung et al. (2025) showed that nitrate-driven eutrophication can alter nitrogen transformations and greenhouse-gas production in coastal lagoons. For Lambayeque, concurrent current, wind, water-column, and drainage observations are needed to distinguish these pathways.

### 4.5 Oceanographic contribution and inferential limitations

The main contribution is a sector-resolved description of recurrent nitrate-DIC-$pCO_2$-$O_2$ covariation along the Lambayeque coast. The four-year monthly record identifies a seasonal nitrate increase, greater persistence in the southern sector, and a recurring inverse nitrate-oxygen relation. These observations extend regional knowledge by defining where and when coordinated marine biogeochemical measurements should be made. They do not provide a land-to-sea mass balance or a mechanistic attribution.

Several limitations illustrate the inferential constraints. The annual land indicators contain four observations and are not significant at $p < 0.05$. Urea imports do not represent field application. The 0.25° product resolution merges the three southern drain outlets. The southern series contains 11 months per year. Monthly correlations use nominal p values without adjustment for temporal autocorrelation, so the effective degrees of freedom may be fewer than the nominal value. The marine fields are model products without in situ validation at the drain outlets. These constraints require interpretation of the results as exploratory co-variation.

### 4.6 Implications for monitoring and management

The results support an ocean-focused monitoring design for the Lambayeque coast. Measurements should target both marine sectors from May to October and should include $NO_3^-$, DIC, total alkalinity, $pCO_2$, chlorophyll a, phytoplankton biomass, NPP, $O_2$, temperature, salinity, currents, and wind. Concurrent drain discharge and nutrient measurements would allow land-derived fluxes to be estimated and separated from upwelling and internal cycling. This design would test the recurrent

https://doi.org/10.5194/egusphere-2026-3633
Preprint. Discussion started: 31 July 2026


nitrate-carbon-oxygen structure identified here and determine whether the southern persistence reflects circulation, retention, external loading, or a combination of processes.

## 5 Conclusions

Surface $NO_3^-$ along the Lambayeque coast showed a recurrent seasonal increase from May to October during 2022-2025. The southern marine sector maintained higher and more persistent values than the northern sector within the Copernicus surface fields.

$NO_3^-$ covaried positively with DIC and $pCO_2$ and inversely with $O_2$ across multiple years. The southern sector showed the most persistent nitrate-carbon-oxygen structure. NPP, chlorophyll a, and phytoplankton carbon were more closely related to $NO_3^-$ in 2024 and 2025 than in the first two years.

The annual relationships with rice production and urea imports were positive but non-significant and contained only four observations. These indicators do not quantify fertiliser application, nitrogen surplus, or land-to-sea flux, and the study does not attribute the marine nitrate pattern to agriculture.

The study identifies an oceanographic pattern that can guide field testing in an under-sampled part of the northern Humboldt system. Coordinated observations of hydrography, currents, nitrate, carbon-system variables, oxygen, biological production, and drain fluxes are required to separate upwelling, retention, internal cycling, and land-derived contributions.

## Code and data availability

The data supporting the reported results are publicly available in Mendeley Data: Hoyos-Alayo, Walter Manuel; Leiva-Piedra, Jorge Luis; Ramirez-Juidiaz, Emilio; Amaro-Mellado, José Lázaro (2026), “Spatiotemporal coupling between rice production, urea use and coastal nitrate dynamics in the marine ecosystem of Lambayeque, Perú”, Mendeley Data, V1, https://doi.org/10.17632/ysjjvnkc22.1.

The supplementary material contains the supporting dataset and complementary information used for the analyses reported in this manuscript. The supplement is provided as a verified ZIP file and is also available through Mendeley Data at https://doi.org/10.17632/ysjjvnkc22.1

## Author contributions

JLL and WMHA conceptualised the study and designed the analytical framework. JLL curated the agricultural and marine data. WMHA and ERJ performed the statistical analysis and interpreted the results. ERJ and JLAM contributed to the methodological review, discussion and manuscript revision. WMHA prepared the manuscript with contributions from all co-authors.

https://doi.org/10.5194/egusphere-2026-3633
Preprint. Discussion started: 31 July 2026


**Competing interests**

The authors declare that they have no conflict of interest.

**Acknowledgements**

The authors appreciate the institutional support provided by the Universidad Tecnológica del Perú and the Universidad de Sevilla during the development of this study.

**Financial support**

No external financial support was reported for this study.

**Review statement**

The review statement will be added by Copernicus Publications listing the handling editor as well as all contributing referees according to their status anonymous or identified.

**References**

Asto, C., Bosse, A., Pietri, A., Sauzède, R., Graco, M., Gutiérrez, D., and Colas, F.: Nutrient estimation in the Peruvian upwelling system based on a neural network approach, Frontiers in Marine Science, 12, 1558747, https://doi.org/10.3389/fmars.2025.1558747, 2025.

Balakrishnan Nair, T. M., Sarma, V. V. S. S., Lotliker, A. A., Muraleedharan, K. R., Samanta, A., Baliarsingh, S. K., Shivaprasad, S., Gireeshkumar, T. R., Raulo, S., Vighneshwar, S. P., Shesu, R. V., Krishna, M., Kumar, N. K., Naik, R. C., Joseph, S., Annapurnaiah, K., Rao, E. P. R., and Srinivasa Kumar, T.: An integrated buoy-satellite based coastal water quality nowcasting system: India's pioneering efforts towards addressing UN ocean decade challenges, Journal of Environmental Management, 354, 120477, https://doi.org/10.1016/j.jenvman.2024.120477, 2024.

Bijay-Singh and Craswell, E.: Fertilizers and nitrate pollution of surface and ground water: An increasingly pervasive global problem, SN Applied Sciences, 3, 518, https://doi.org/10.1007/s42452-021-04521-8, 2021.

Brando, V. E., Santoleri, R., Colella, S., Volpe, G., and Di Cicco, A.: Overview of operational global and regional ocean colour essential ocean variables within the Copernicus Marine Service, Remote Sensing, 16, 4588, https://doi.org/10.3390/rs16234588, 2024.

https://doi.org/10.5194/egusphere-2026-3633
Preprint. Discussion started: 31 July 2026


Cheung, H. L. S., Zilius, M., Politi, T., Lorre, E., Vybernaite-Lubiene, I., Santos, I. R., and Bonaglia, S.: Nitrate-driven eutrophication supports high nitrous oxide production and emission in coastal lagoons, Journal of Geophysical Research: Biogeosciences, 130, e2024JG008510, https://doi.org/10.1029/2024JG008510, 2025.

Cossarini, G., Feudale, L., Teruzzi, A., Bolzon, G., Coidessa, G., Solidoro, C., Di Biagio, V., Amadio, M., Lazzari, P., Brosich, A., and Salon, S.: High-resolution reanalysis of the Mediterranean Sea biogeochemistry (1999–2019), Frontiers in Marine Science, 8, 741486, https://doi.org/10.3389/fmars.2021.741486, 2021.

E.U. Copernicus Marine Service Information: Global Ocean Biogeochemistry Analysis and Forecast (GLOBAL_ANALYSISFORECAST_BGC_001_028), Copernicus Marine Service [data set], https://doi.org/10.48670/moi-00015, 2026.

Farias, L. and de la Maza, L.: Understanding the impacts of coastal deoxygenation in nitrogen dynamics: An observational analysis, Scientific Reports, 14, 11826, https://doi.org/10.1038/s41598-024-62186-w, 2024.

Gbedourorou, S. K., Tovihoudji, P. G., Zakari, S., Vanclooster, M., and Akponikpè, P. B. I.: Effect of water-saving technologies on nitrogen losses in rice fields: A meta-analysis, Agricultural Water Management, 312, 109400, https://doi.org/10.1016/j.agwat.2025.109400, 2025.

Kessouri, F., McWilliams, J. C., Bianchi, D., Sutula, M., Renault, L., Deutsch, C., Feely, R. A., McLaughlin, K., Ho, M., Howard, E. M., Bednaršek, N., Damien, P., Molemaker, J., and Weisberg, S. B.: Coastal eutrophication drives acidification, oxygen loss, and ecosystem change in a major oceanic upwelling system, Proceedings of the National Academy of Sciences of the United States of America, 118, e2018856118, https://doi.org/10.1073/pnas.2018856118, 2021.

Kittu, L. R., Paul, A. J., Fernández-Méndez, M., Hopwood, M. J., and Riebesell, U.: Coastal $N_2$ fixation rates coincide spatially with nitrogen loss in the Humboldt Upwelling System off Peru, Global Biogeochemical Cycles, 37, e2022GB007578, https://doi.org/10.1029/2022GB007578, 2023.

Lachkar, Z., Cornejo-D'Ottone, M., Singh, A., Arístegui, J., Dewitte, B., Fawcett, S., Garçon, V., Lovecchio, E., Molina, V., and Vinayachandran, P. N. M.: Biogeochemistry of greenhouse gases in coastal upwelling systems: Processes and sensitivity to global change, Elementa: Science of the Anthropocene, 12, 00088, https://doi.org/10.1525/elementa.2023.00088, 2024.

Li, X., Zheng, H., Mao, Z., Du, P., and Zhang, W.: Change in water column total chlorophyll-a in the Mediterranean revealed by satellite observation, Science of the Total Environment, 945, 174076, https://doi.org/10.1016/j.scitotenv.2024.174076, 2024.

Min, J., Sun, H., Wang, Y., Pan, Y., Kronzucker, H. J., Zhao, D., and Shi, W.: Mechanical side-deep fertilization mitigates ammonia volatilization and nitrogen runoff and increases profitability in rice production independent of fertilizer type and split ratio, Journal of Cleaner Production, 316, 128370, https://doi.org/10.1016/j.jclepro.2021.128370, 2021.

Paparazzo, F. E., Fernandez-Severini, M. D., Pierattini-Martinez, R., Silva, R., Ardusso, M., Bermejo, P., and Reta, R.: Marine coastal chemistry related to inland inputs in San Jorge gulf and the adjacent north coast, Science of the Total Environment, 947, 174488, https://doi.org/10.1016/j.scitotenv.2024.174488, 2024.

https://doi.org/10.5194/egusphere-2026-3633
Preprint. Discussion started: 31 July 2026


Peñuelas, J., Coello, F., and Sardans, J.: A better use of fertilizers is needed for global food security and environmental sustainability, Agriculture & Food Security, 12, 5, https://doi.org/10.1186/s40066-023-00409-5, 2023.

Santos-Bruña, J. J., Hernández-Hernández, N., Montero, M. F., Gómez-Letona, M., Baumann, M., Taucher, J., Spisla, C., Thielecke, A., Ludwig, A., Riebesell, U., and Arístegui, J.: Assessment of potential eutrophication in coastal waters of Gran Canaria: Impact on plankton community under $CO_2$ depletion, Marine Environmental Research, 204, 106919, https://doi.org/10.1016/j.marenvres.2024.106919, 2025.

Wang, L., Shang, S., Liu, W., She, D., Hu, W., and Liu, Y.: Hydrodynamic controls on nitrogen distribution and removal in aquatic ecosystems, Water Research, 242, 120257, https://doi.org/10.1016/j.watres.2023.120257, 2023.

Wang, X., Zhu, H., Hou, S., Cui, H., and Yan, B.: Environmental impacts of fertilization during rice production in saline-alkali paddy fields based on life cycle assessment, Journal of Cleaner Production, 467, 142947, https://doi.org/10.1016/j.jclepro.2024.142947, 2024.

Yari, S., Mohrholz, V., and Bordbar, M. H.: Wind variability across the North Humboldt Upwelling System, Frontiers in Marine Science, 10, 1087980, https://doi.org/10.3389/fmars.2023.1087980, 2023.

Zhang, W.: Unexpected high indirect impacts of riverine organic matter to coastal deoxygenation, Water Research, 225, 119180, https://doi.org/10.1016/j.watres.2022.119180, 2022.

Zhong, X., Zhou, X., Luo, G., Huang, Y., Wu, Y., Cao, R., Tian, C., and Peng, J.: Soil mineral nitrogen, soil urease activity, nitrogen losses and nitrogen footprint under machine-planted rice with side-deep fertilization, Plant and Soil, 494, 185–202, https://doi.org/10.1007/s11104-023-06263-5, 2024.